June 2021

Heat and fluid flow downstream of a row of finite-height circular cylinders

Saarah Akhand
University of Windsor, akhand11@uwindsor.ca

Heat and fluid flow downstream of a row of finite-height circular cylinders

By

Saarah Akhand

A Major Research Paper
Submitted to the Faculty of Graduate Studies
through the Department of Mechanical, Automotive and Materials Engineering
in Partial Fulfillment of the Requirements for
the Degree of Master of Applied Science
at the University of Windsor

Windsor, Ontario, Canada

2021

Heat and fluid flow downstream of a row of finite-height circular cylinders

by

Saarah Akhand

APPROVED BY:

_____
N. Eaves
Department of Mechanical, Automotive and Materials Engineering

_____
G. Reader, Co-Advisor
Department of Mechanical, Automotive and Materials Engineering

_____
D. Ting, Co-Advisor
Department of Mechanical, Automotive and Materials Engineering

May 31, 2021

DECLARATION OF ORIGINALITY

I hereby certify that I am the sole author of this major paper and that no part of this major paper has been published or submitted for publication.

I certify that, to the best of my knowledge, my major paper does not infringe upon anyone's copyright nor violate any proprietary rights and that any ideas, techniques, quotations, or any other material from the work of other people included in my major paper, published or otherwise, are fully acknowledged in accordance with the standard referencing practices. Furthermore, to the extent that I have included copyrighted material that surpasses the bounds of fair dealing within the meaning of the Canada Copyright Act, I certify that I have obtained a written permission from the copyright owner(s) to include such material(s) in my major paper and have included copies of such copyright clearances to my appendix.

I declare that this is a true copy of my major paper, including any final revisions, as approved by my thesis committee and the Graduate Studies office, and that this major paper has not been submitted for a higher degree to any other University or Institution.

ABSTRACT

Induced turbulence created by a row of finite height cylinders is applicable in different engineering applications, e.g., for promoting convective cooling of solar panel. In this study, flow past a row of 13 side-by-side finite-height circular cylinders having a height-diameter (h/d) ratio of 2 (20mm/10mm) and center to center distance between adjacent cylinders (g) of 2d was scrutinized at a Reynolds number based on cylinder height of 4700 inside a wind tunnel over a flat plate. The flow at 5h and 10h downstream of the cylinder array was characterized using a 2-d hot wire anemometer. To understand the convective heat transfer from the hot plate, Nusselt number normalized by the reference no-cylinder case, Nu/Nu_0, was deduced based on the temperature difference between the lower and upper surfaces of the hot plate. Significant heat transfer enhancement occurred which was explained in terms of flow properties. A regression analysis was performed, and it was revealed that the most influential parameters for enhancing heat transfer were the stream-wise turbulent intensity followed by the stream-wise velocity.

DEDICATION

To my parents Major Mubassher (retd), Shampa Chowdhury

and my brother Lt. Mushabbir.

ACKNOWLEDGEMENTS

TABLE OF CONTENTS

LIST OF TABLES

LIST OF FIGURES

LIST OF APPENDICES

NOMENCLATURE

A	Local heat transfer area (mm^2)
B	Bias uncertainty
d	Diameter of the cylinder (mm)
g	Gap spacing (Center to center distance of two adjacent cylinders; mm)
h	Height of the cylinder (mm)
H	Convective heat transfer coefficient
h/d	Aspect ratio (cylinder height/ cylinder diameter)
k_{PTFE}	Conductivity of the plate (W/m·K)
N	Sampling number
Nu	Nusselt number
Nu_0	Unperturbed reference Nusselt number
P	Precision uncertainty
$PTFE$	Polytetrafluoroethylene
$\dot{Q}_{convection}$	Convective heat transfer rate (W)

$\dot{Q}_{radiation}$	Radiative heat transfer rate (W)
$\dot{Q}_{Total}$	Total heat transfer rate (W)
Re	Reynolds number based on the cylinder height
$stdj$	Standard deviation of studied individual parameters.
$stdy$	Standard deviation of the dependent variable (Nu/Nu_0)
T_{Air}	Surrounding air temperature (K)
T_{Bottom}	Bottom surface temperature (K)
T_{Top}	Top surface temperature (K)
T_{Wall}	Wall temperature (K)
Tu	Stream-wise turbulence intensity
u_{rms}	Root-mean-square velocity in the X direction (m/s)
v_{rms}	Root-mean-square velocity in the Y direction (m/s)
u_i	Instantaneous fluctuating velocity in the X direction (m/s)
U_i	Instantaneous velocities in the X direction (m/s)

$\overline{U}$	Time-averaged local velocity in the X direction (m/s)
U_∞	Time-averaged free-stream velocity (m/s)
v_i	Instantaneous fluctuating velocity in the Y direction (m/s)
V_i	Instantaneous velocities in the Y direction (m/s)
$\overline{V}$	Time-averaged velocity in the Y direction (m/s)
X	Streamwise direction
Y	Cross-stream direction
Z	Vertical direction
β_j	Regression coefficient
$\beta_j{}^{std}$	Standardized regression coefficient
ε	Emissivity

CHAPTER 1

INTRODUCTION

1.1 Motivation and Background

Effectiveness of the convective heat transfer by air is important in many engineering applications. Various methods have been investigated for enhancing convective heat transfer and they can be categorized as active, passive, or compound [1]. Efforts to enhance heat transfer via active means such as mechanical devices, electric or acoustic fields require external power, whereas passive methods enhance heat transfer by manipulating surface geometry to increase flow. Some examples of active methods include jet impingement, flow alteration, vibration, water spray etc. [2-4]. A notable downside of the active cooling method is the requirement of external power along with higher initial expenditure. In contrast, a passive method is a much simpler approach for enhancing heat convection. These passive methods can help boosting energy conversion efficiency of various renewable energy systems like solar thermal or solar photovoltaic.

Different types of turbulent generators (TG) such as grid, rib, winglet, strip, and cylinder have been used as passive cooling device to enhance heat transfer via the resulting flow turbulence and vorticity.[5-6] Among these vortex generators, finite height cylinder is a very promising one because of its end effects. The free end of the short cylinder can contribute to the downwashed flow behind the cylinder which effects the heat transfer properties. [7] Because of its simple geometry a lot of investigations have been done by using more than one cylinder as multiple cylinders in proximity to one another is of practical importance in many engineering applications. A number of studies have been conducted on the heat transfer augmentation caused by multiple cylinders in different

geometrical arrangements [8-11]. For the better understanding of the effect of a row of finite height cylinders on convective cooling of solar panel, an experimental research on unconfined flat surface should be conducted.

1.2 Literature Review

Because of its complex flow mechanism and numerous practical applications, flow over multiple cylinders have been vastly investigated both experimentally and numerically. A summary of studies using a row of side-by-side cylinders is presented in Table 1.1. In 1975, Ishigai and Nishikawa conducted an experimental study using a single row of cylinder on a flat plate by varying gap size among the cylinders over a range of Reynolds numbers between 4000 and 9500 [12]. They observed that basic properties of vortex formation region highly depend on gap spacing between cylinders. When the gap spacing is less than 2.5d (d =diameter of the tube) vortex formation region occurs both in larger and smaller wakes whereas for gap spacing less than 1.5d vortices were only formed in the smaller wakes. In 1996, another study conducted a numerical investigation at a lower Reynolds number of 120 by using boundary fitting coordinate system on an array consisting of 7 cylinders to understand the effect of different gap spacing, 2d, 2.5d, and 3.3d, on a cylinder array [13]. An improvement in heat transfer rate was observed with decreasing gap between the cylinders due to the increase in local velocities of fluid around the cylinder. Sumner et al. [14] worked with two and three side by side cylinders in a row with different gap spacing and a Reynolds number of 3000 to observe their effect on flow properties. They observed three different flow patterns by varying the gap spacing. Single bluff-body flow for small gap spacing (g ≤1.25d), Biased synchronized shedding for intermediate gap spacing (g >1.25d) and symmetric synchronized shedding higher gap

spacing (g >1.5d). The strength of vortices behind the cylinder array increases with decreasing gap spacing between them.

Cheng et al. [15] also investigated the effect of a row of cylinder over a flat plate on flow properties with a Reynolds number of 2500 and a gap spacing of 1.3d, 2.3d. Maximum Turbulent intensity was being observed just after crossing the tubes and decreases by moving towards downstream distances. A range of different number of tubes (2,3,4,5) in n row had been used to see the effect of number of tubes on heat transfer augmentation [16]. Two sets of experiment have been conducted with and without the effect of a 5mm rod behind the tubes. Two different gaps spacing 1.5d,3d and a much higher Reynolds number, Re=21000 had been used in their study. Their study shows that the heat transfer performance increases with increasing number of tubes and gap spacing. Kang et al [17] performed a numerical investigation by varying g (gap spacing) between the cylinder for a lower Reynolds number, Re=100. In their study they observed five different wake patterns over the flow range by varying g 1.3d,1.8d,2.2d,2.5d,3d,4d,5d When g>2.2d larger vortex shedding has been noticed. Effect of Reynold number on heat transfer performance by an array of cylinder were studied for a range of low Reynolds number of Re=20-180 [18]. Nine different Reynolds numbers were numerically studied with a gap spacing of 2.5d. They observed an increase in heat transfer performance with increasing Reynolds number. Silva et al. [19] numerically investigated the effect of an array of cylinders on convective heat transfer by using immerse boundary method. They worked with a range of aspect ratio, gap spacing and number of cylinders. The wake structure and their interaction between cylinders were studied to identify their effect of heat transfer augmentation. Heat transfer performance increases with increasing number of cylinders

and decreasing gap spacing for g less than 2.1d. The maximum Nusselt number was observed while using the maximum number of cylinders, 10, by maintaining a center-to-center distance of 1.5d.

Table 1.1. Summary of side-by-side cylinders in a single row

Authors	Method used	Parameters	Remarks
Ishigai et al. [12]	Flow visualization method (Forced convection)	Re= Between 4000-9500 h/d= 1.25,1.5,2,2.5 (aspect ratio) g= 1.25d,1.5d,2d,2.5d (center to center distance) Number of tubes used = 5	Vortex formation region depends on tube spacing. g <2.5d vortex formation region occurs in both larger and smaller wakes. g < 1.5d vortex formation region occurs in smaller wakes.
Yamamoto et al. [13]	Boundary fitted coordinate system. (Forced convection)	Re= 120 h/d= 11 g= 2d, 2.5d, 3.3d Number of tubes used = 7	Heat transfer rate improves with decreasing gap between cylinders.
Sumner et al. [14]	Flow visualization method (Forced convection)	Re=3000 g=1.125d,1.25d,1.5d, 2d, 2.5d h/d =16 Number of cylinders used =3	Strength of vortices increases with decreasing g (g<1.5).
Cheng et al. [15]	Wind Tunnel Hot wire anemometer (Forced convection)	Re=2500 h/d= 18 g= 1.3d, 2.3d Number of tubes used= undefined	Max Turbulent intensity was being observed just after crossing the tubes and decreases by moving towards downstream distances.
Tsutsui et al. [16]	Flow visualization smoke wire method	Re= 21000 g = 1.5d, 3d h/d=20	Heat transfer performance increases with increasing number of tubes.
Kang et al. [17]	Immerse Boundary Method (IBM)	Re= 100 g=1.3d,1.8d,2.2d,2.5d,3d,4d,5d h/d=Undefine Number of cylinders= 3	Larger vortex shedding has been noticed when g > 2.2d.
Cho et al. [18]	Immerse Boundary Method (IBM)	Re=20,40,60,80,100,120,140,160,180 g=2.5d h/d= Undefine Number of cylinders used= 8	The heat transfer performance improves with increasing Reynolds Number.
Silva et al. [19]	Immersed Boundary Method (IBM) (Forced convection)	Re=150 g= 1.2d, 1.5d 2.1d,2.4d h/d= 0.4~5.2 Number of cylinders= 6,7,8,9,10	Heat transfer performance increases with increasing number of cylinders. Increases when g < 2.1d Max at g = 1.5d for all number of cylinders.

Different types of experiments had been conducted on a side-by-side array of cylinder by varying parameters like gap spacing, Reynolds number and aspect ratio. Reynolds number for these studies have been measured by based on two different parameters e.g., Cylinder diameter [14-16] and channel size [12-13,17-19]. Channel Reynolds number can specify the significance of inertial effects in the free regions where the cylinder has been kept. Whereas diameter-based Reynolds number can predict the onset of the vortex shedding from the cylinder [20]. In this study, to understand the flow field behind the cylinder on a flat plate, diameter-based Reynolds number has been considered. Studies regarding lower Reynolds number has been considered in this literature review to understand the effect of gap spacing and number of cylinders in a row for different range of Reynolds number and to find out moderate gap spacing and number of cylinders for this study. Some studies performed experimental methods while others are based on numerical methodologies. Some of these experimental studies had been conducted on a flat plate[12,15]. A row of finite cylinders on a flat plate can be very promising to enhance the heat transfer to a significant amount.

1.3 Research Objective

This study investigates the flow properties and heat transfer enhancement of a row of finite height cylinders on an unconfined flat plate. A row of 13 cylinders with an aspect ratio (height/diameter) of 2 (20mm/10mm) and gap spacing (diameter to diameter distance) of 2d was investigated at a Reynolds number of 4700 (based on diameter). The most effective flow parameters behind the heat transfer augmentation are deduced via a regression analysis.

References

[1] Webb, R. (1994). Principles of enhanced heat transfer. New York: John Wiley & Sons. doi.org/10.1016/0140-7007(95)90013-6.

[2] Esfe, M. H., Kamyab, M. H., & Valadkhani, M. (2020). Application of nanofluids and fluids in photovoltaic thermal system: An updated review. Solar Energy, 199, 796-818.

[3] Liu, S., & Sakr, M. (2013). A comprehensive review on passive heat transfer enhancements in pipe exchangers. Renewable and Sustainable Energy Reviews, 19, 64-81.

[4] Nižetić, S., Čoko, D., Yadav, A., & Grubišić-Čabo, F. (2016). Water spray cooling technique applied on a photovoltaic panel: The performance response. Energy Conversion and Management, 108, 287-296.

[5] Yang, Y., Ting, D. S. K., & Ray, S. (2020). Heat transfer enhancement of a heated flat surface via a flexible strip pair. International Journal of Heat and Mass Transfer, 159. 120-139.

[6] Wu, H., Ting, D. S. K., Ray, S. (2018). The effect of delta winglet attack angle on the heat transfer performance of a flat surface. International Journal of Heat and Mass Transfer, 120, 117–126.

[7] García-Villalba, M., Palau-Salvador, G., & Rodi, W. (2014). Forced convection heat transfer from a finite-height cylinder. Flow, turbulence and combustion, 93(1), 171-187.

[8] Buyruk, E. (2002). Numerical study of heat transfer characteristics on tandem cylinders, inline and staggered tube banks in crossflow of air. International Communications in Heat and Mass Transfer, 29(3), 355-366.

[9] Horvat, A., & Mavko, B. (2006). Heat transfer conditions in flow across a bundle of cylindrical and ellipsoidal tubes. Numerical Heat Transfer, Part A: Applications, 49(7), 699-715.

[10] Liang, C., Papadakis, G., & Luo, X. (2009). Effect of tube spacing on the vortex shedding characteristics of laminar flow past an inline tube array: a numerical study. Computers & Fluids, 38(4), 950-964.

[11] Huang, Z., Olson, J. A., Kerekes, R. J., & Green, S. I. (2006). Numerical simulation of the flow around rows of cylinders. Computers & Fluids, 35(5), 485-491.

[12] Ishigai, S. and Nishikawa, E. (1975) Experimental study of structure of gas flow in tube banks with tube axes normal to flow, Part II. On the structure of gas flow in single-column, single-row, and double rows tube banks. Bull JSME, vol.18, no. 119, pp. 528–535.

[13] Yamamoto, H. and Hattori, N. (1998). Flow and heat transfer around a single row of circular cylinders. Heat Transfer‑Japanese Research: Co‑sponsored by the Society of Chemical Engineers of Japan and the Heat Transfer Division of ASME, 25(3), 192-200.

[14] Sumner, D., Wong, S. S. T., Price, S. J., & Paidoussis, M. P. (1999). Fluid behavior of side-by-side circular cylinders in steady crossflow. Journal of Fluids and Structures, 13(3), 309-338.

[15] Cheng, M., & Moretti, P. M. (1988). Experimental study of the flow field downstream of a single tube row. Experimental Thermal and Fluid Science, 1(1), 69-74.

[16] Tsutsui, T. (2017). Heat transfer enhancement of a single row of tube. In EPJ Web of Conferences (Vol. 143, p. 02132). EDP Sciences.

[17] Kang, S. (2004). Numerical study on laminar flow over three side-by-side cylinders. KSME international journal, 18(10), 1869-1879.

[18] Cho, J., & Son, C. (2008). A numerical study of the fluid flow and heat transfer around a single row of tubes in a channel using immerse boundary method. Journal of mechanical science and technology, 22(9), 1808-1820.

[19] Silva, A. L. E. (2014). Convection heat transfer around a single row of cylinders. Computational Thermal Sciences, 6 (6): 477–492.

[20] Shahsavari, S., Wardle, B. L., & McKinley, G. H. (2014). Interception efficiency in two-dimensional flow past confined porous cylinders. Chemical Engineering Science, 116, 752-762.

CHAPTER 2

Experimentation and Data Analysis

This research was carried out in the turbulence and energy laboratory located in the engineering building at the University of Windsor. The Experimental setup for this research has been conducted in two parts. Detailed flow and heat transfer characteristics of an array of finite height cylinders has been studied inside a wind tunnel. The whole experimental setup and procedure will be discussed in this chapter.

2.1 The Experimental Setup

In this present study, experiments have been performed to determine flow and heat transfer characteristics of an array of finite height cylinders situated inside a wind tunnel. The model chosen for this research can be seen in Figure 2.1. A total thirteen 20mm height and 10mm diameter cylinders have been used by maintaining aspect ratio h/d=2 where g=2d diameter-to-diameter distance have been kept between the cylinders. An increase in heat transfer augmentation has been observed with decreasing gap between cylinder (when g<2.1d) and increasing number of cylinders in an array [1-3].
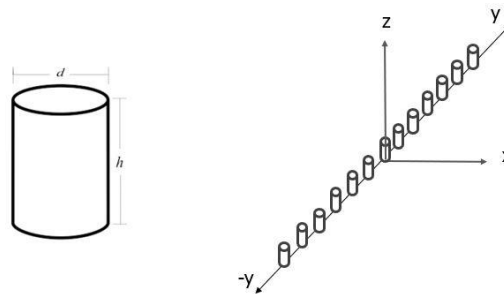
Figure 2.1: Experimental model

2.2 Experimental flow facility

The whole experiment has been conducted inside a wind tunnel having a cross section of 76cm x 76cm. The entire setup to acquire flow measurement data is composed of a hotwire probe, a temperature probe, a constant temperature hotwire anemometer (CTA) and Stream-Ware application software. In this study turbulent quantities are measured by using a 2D hotwire probe (type 55R51). A temperature probe is placed with the hotwire probe to get the value of air temperature and makes corrections to the hot wire calibration coefficient. To ensure accurate data acquisition hotwire probe was calibrated before carrying out each set of data. Two types of calibrations: velocity and directional calibration were performed. After the calibration was done probe is then placed inside the wind tunnel. A 295 mm wide,380 long mm and 3 mm thick PTFE (Polytetrafluoroethylene) plate is located inside the wind tunnel, on the surface of that PTEE plate the cylinders have been placed facing the hotwire probe by maintaining downstream distance 5h (100mm) and 10h (200mm) to get two sets data. Figure 2.2 shows the experimental setup and details of the test facilities. The test started by setting the mean velocity (in this case 7m/s) corresponding to the preset Reynolds number (4700). The probe holder was then moved to the positions where actual data collection was required. At each point, a raw data is being generated which is then acquire and reduced with the help of Stream-Ware software. Those reduced data containing flow characteristics like turbulent intensity, Taylor microscale were then exported and used to make desired graphs. Following the procedure according to ref [4] instantaneous velocities were deducted from the measured voltages over a 90mm×40mm grid with a resolution of 4mm.
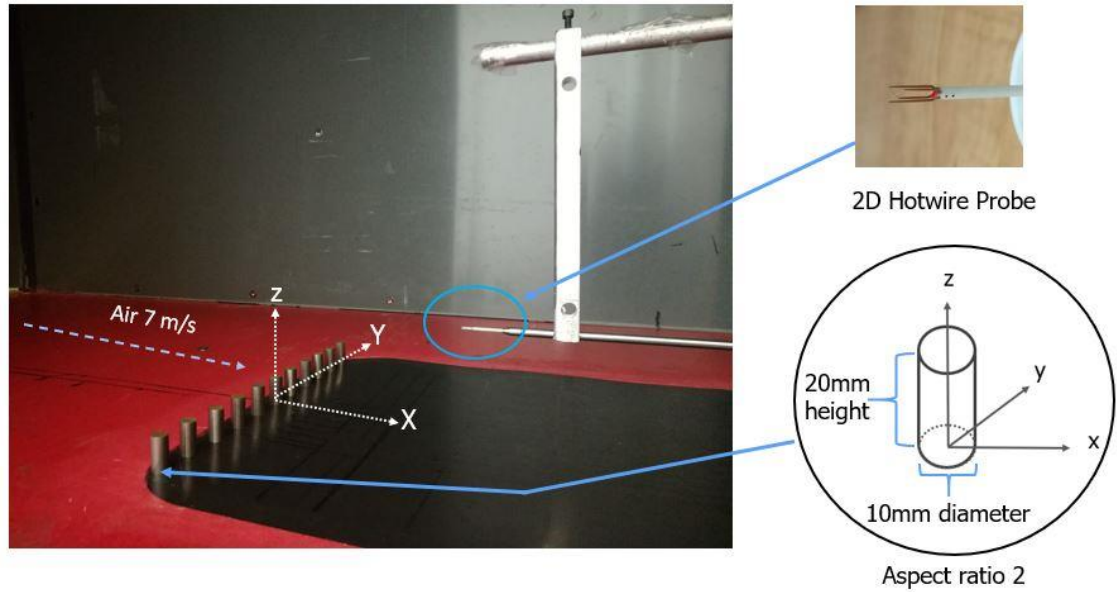
Figure 2.2: Experimental flow facility

2.3 Heat Transfer Data Acquisition

Inside the 76cm x 76 cm cross section of the wind tunnel 13 number of cylinders in an array orientation was placed over a 295 mm wide and 380mm long PTFE (polytetrafluoroethylene) plate. The PTFE plate has a thickness of 3mm. The conductivity of the PTFE plate was 0.25 W/ (m.K) and the emissivity of the plate was 0.92. A water tank was placed underneath the PTFE plate. The function of the water tank was to generate steam to maintain the bottom of the PTFE plate temperature at 100°C. A FlirC2 thermal camera had been used by a K type thermocouple with an accuracy of 0.5°C. The resolution of the camera was 60x80 pixels. The camera is positioned 0.5m above the heated PTFE plate on top section of the wind tunnel.

By using the camera, the convective heat transfer enhancement of the top surface of PTFE plate was deduced with and without the cylinders array. The temperature distribution along PTFE plate was captured. The Nusselt number was normalized by the reference Nusselt

number without the cylinder array. Figure 2.3 shows the experimental setup and details of the heat transfer data acquisition test facilities.
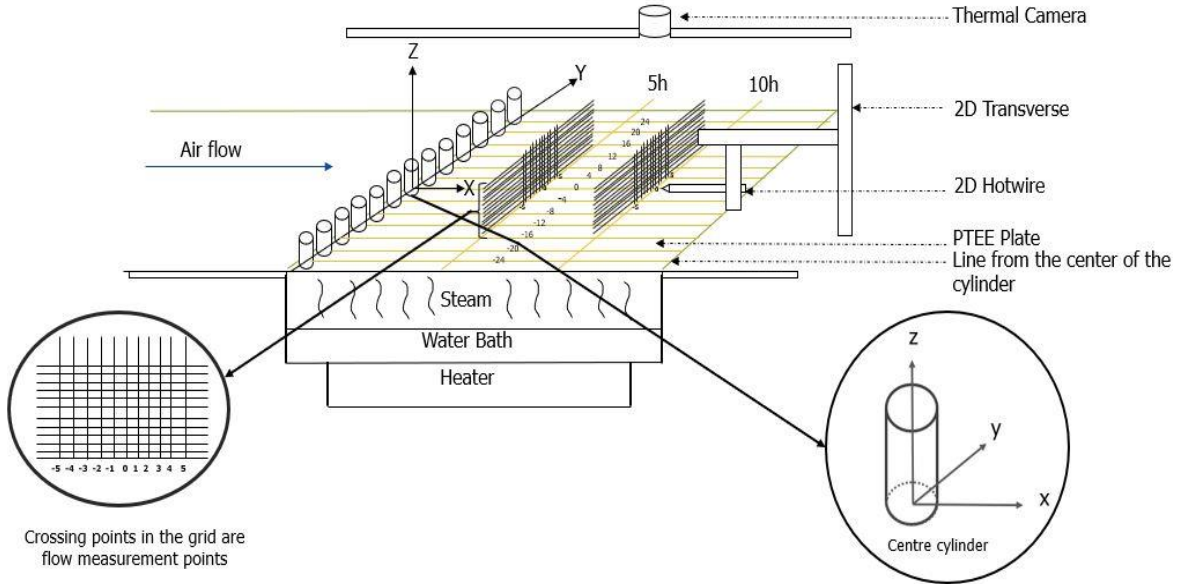
Figure 2.3: Experimental setup for heat transfer data acquisition

2.4 Data Analysis

The total heat Transfer rate from the PTFE plate contains the types of heat transfer, mainly convection, a small amount of radiation and a negligible amount of conduction. The convective heat transfer rate of the PTFE plate can be determined as

$$\dot{Q}_{convention} = \dot{Q}_{total} - \dot{Q}_{radiation} \tag{1}$$

The total heat transfer rate can be calculated using :

$$\dot{Q}_{total} = \frac{K_{PTFE} \cdot A(T_B - T_T)}{T_{PTFE}} \tag{2}$$

Here, the PTEE plate conductivity K_{PTFE} as 0.25 W/(m·K), the thickness of the plate as 3mm, area of the plate A = 295 mm by 380 mm, the temperature of the bottom surface, T_B was 100°C, and the top surface temperature, T_T was measured by the thermal camera.

The rate of heat radiated to the surrounding can be deduced from:

$$\dot{Q}_{Radiation} = \varepsilon\sigma A(T_{top}^4 - T_{surrounding}^4) \qquad (3)$$

Here, Emissivity ε = 0.92 [5] ,the Boltzmann's constant, σ, was $5.67 \times 10^{-8} Wm^{-2}K^{-4}$ [6], and the surrounding temperature, $T_{surrounding}$, was approximately 295 K.

The convection heat transfer coefficient is defined as:

$$h_{convention} = \frac{\dot{Q}_{Convection}}{A\,(T_{top} - T_{surrounding})} \qquad (4)$$

So, the corresponding non-dimensional Nusselt number is:

$$Nu = \frac{h_{convention}}{P_{Air}} \qquad (5)$$

The final approach is to get the normalized Nusselt number which is basically the relation between non-dimensional Nusselt number and local Nusselt number without the array of cylinders.

$$\frac{Nu}{Nu_0} = \frac{h}{h_0} \qquad (6)$$

In addition to local heat transfer enhancement, the overall enhancement of the entire plate is also of importance. The span averaged values should be appropriately calculated as per equation 7. Here P denotes the parameter of interest i.e., the normalized Nusselt number

and n denotes the number of span-averaging values. The value of n is chosen to be 20 for the span-averaged Nu/Nu_0 profile.

$$\bar{P} = \frac{1}{n}\sum_1^n P_i \tag{7}$$

The time-averaged velocity can be obtained from equation 8, where $N=10^6$ is the sample size, where U_i and V_i, are streamwise, width wise and vertical velocities.

$$\bar{U} = \frac{1}{N}\sum_{i=1}^N U_i \; ; \; \bar{V} = \frac{1}{N}\sum_{i=1}^N V_i; \tag{8}$$

By subtracting the time-averaged velocity from instantaneous velocity, the instantaneous fluctuating velocity is obtained as $u_i = U_i - \bar{U}$, $v_i = V_i - \bar{V}$ from which the root-mean-square fluctuating velocity can be calculated from equation 9,

$$u_{rms} = \sqrt{\sum_{i=1}^N \frac{u_i^2}{N-1}} \tag{9}$$

Once, the u_{rms} value is calculated, from there the local turbulent intensity is calculated by normalizing the u_{rms} by free stream velocity U_∞

$$Tu = \frac{u_{rms}}{U_\infty} \tag{10}$$

The small eddies in the turbulent and actively kinetic energy dissipating via viscosity can be represented by Taylor microscale. Taylor time scale (τ_λ) can be expressed as:

$$\tau_\lambda = \sqrt{\frac{\overline{2u_i^2}}{\overline{(\frac{du_i}{dt})^2}}} \tag{11}$$

14

When the data is discrete,

$$\tau_\lambda = \sqrt{\frac{\frac{1}{N}\Sigma_{i=1}^{N} 2u_i^2}{\frac{1}{N-1}\Sigma_{i=1}^{N-1}(\frac{u_{i+1}-u_i}{\Delta t})^2}} \qquad (12)$$

Taylor micro-scale can be obtained:

$$\lambda = \overline{U}\tau_\lambda \qquad (13)$$

Due to the random variations when the acquisition of the instantaneous velocity data was taken through hot wire precision (P) uncertainty occur. By following the process from ref [7] total uncertainty of each flow parameter consisting of some bias uncertainty (B) was calculated, see appendix A.

To find out the effect of stream-wise velocity, $\overline{U}/U_\infty$ and local vertical turbulent intensity, U_{rms}/U_∞, streamwise Taylor microscale, λ/h, on heat transfer enhancement, Nu/Nu_0 we performed multiple linear regression analysis. To find the weight of impact, the standardized regression coefficients ($\beta_j{}^{std}$) were used [8]:

$$\beta_j{}^{std} = \beta_j \frac{std_j}{std_y} \qquad (14)$$

Here, β_{jstd} represents the standardized regression coefficient, which indicates the impact of the individual studied flow parameters ($\overline{U}/U_\infty$, U_{rms}/U_∞, λ/h) on the dependent variable (Nu/Nu_0), β_j and std_j are the regression coefficient and standard deviation of each of the studied individual parameter where std_y is the standard deviation of the dependent variable (Nu/Nu_0).

Reference

[1] Yamamoto, H. and Hattori, N. (1998). Flow and heat transfer around a single row of circular cylinders. Heat Transfer-Japanese Research: Co-sponsored by the Society of Chemical Engineers of Japan and the Heat Transfer Division of ASME, 25(3), 192-200.

[2] Silva, A. L. E. (2014). Convection heat transfer around a single row of cylinders. Computational Thermal Sciences, 6 (6): 477–492.

[3] Tsutsui, T. (2017). Heat transfer enhancement of a single row of tube. In EPJ Web of Conferences (Vol. 143, p. 02132). EDP Sciences.

[4] Jørgensen, F. E. (2005). How to Measure Turbulence with Hot-Wire Anemometers: A Practical Guide. Dantec dynamics.

[5] "Emissivity Coefficients Materials." [Online]. Available: https://www. engineeringtoolbox.com/emissivity-coefficients-d_447.html. [Accessed: 10- May-2021].

[6] "Radiation Heat Transfer." [Online]. Available: https://www.engineeringtoolbox. com/radiation-heat-transfer-d_431.html. [Accessed: 10-May-2021].

[7] Figliola, R. S., & Beasley, D. E. (2001). Theory and design for mechanical measurements.

[8] Myers, J. L., Well, A., Lorch, R. F. (2010). Research design and statistical analysis. Routledge.

CHAPTER 3

Result and Discussion

To determine the effect of an array of finite height cylinders on the fluid flow downstream the turbulence in the flow field was studied in term of velocity, turbulence intensity and Taylor microscale. Also, the temperature distribution along the PTEE (Polytetrafluoroethylene) plate from an array of finite height cylinders by maintain 1h distance between them was captured. Those data were then studied to measure the effect of distance between cylinders in thermal performance. A normalised Nusselt number was then obtained from those measurements. Later, flow measurement captured at 5h and 10h vortical flow downstream was then explained with the help of heat transfer behaviour due to this specifically arranged array of cylinders. This chapter presents an elaborate discussion of flow properties and heat transfer enhancement from an array of cylinders.

3.1 Effect of a row of finite height cylinders on convection heat transfer

The effect of a side-by-side array of cylinders on the augmentation of forced convection over the heated PTEE plate has been examined. A normalized Nusselt number has been obtained by normalize the local Nusselt number with the help of reference Nusselt number without the cylinder array. Correlation at 5h and 10h downstream of the cylinder array over the flat plate has been determined for quasi-steady flow.

Figure 3.1 represents the normalized Nusselt number, *Nu/Nu$_0$* distribution of the PTFE plate. The dotted semicircles denote the center three cylinders of the cylinder array which falls between (*Y*=±1.25*h*). The uncertainty of *Nu/Nu$_0$* was around 0.062. The region near

the cylinder array represented highest normalized Nusselt number, Nu/Nu_0 value. Cylinder array behaved like fins could be possible explanation behind this reaction. Another possible explanation behind this behavior is the intense velocity fluctuation and turbulence field just after crossing the cylinder due to the end effect of finite height of the cylinder [1]. On that region the cylinder array resulted higher $Nu/Nu_0 = 1.68$. After crossing the cylinders as the fluid is flowing towards downstream over the flat plate and picking up thermal energy from the plate along its way there is a decrease of $Nu/Nu_0 = 1.27$ at X=20h occurs over the flat plate as we are moving away from the cylinder which follows the similar pattern of the existing numerical study of Silva et.al [2]. To understand this behavior more precisely cross-sectional Nu/Nu_0 profile at various downstream distances needs to be examined.
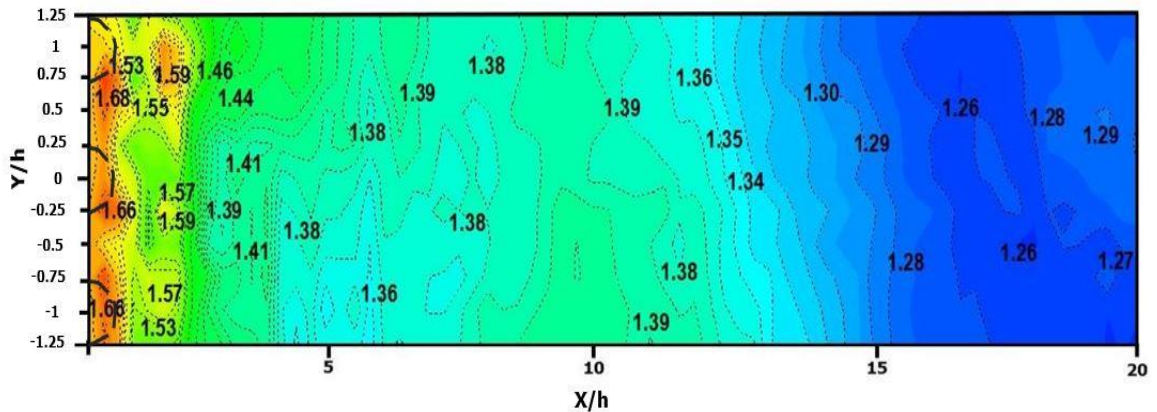
Figure 3.1: The normalized Nusselt number, Nu/Nu_0, distribution of an array of cylinder

Figure 3.2 represents the effect an array of cylinders on the cross-sectional Nu/Nu_0 profile at various downstream distances. It is noted that at X=5h downstream distance the peak Nu/Nu_0 is nearly 1.4 which is higher than the peak of Nu/Nu_0 at X=10h downstream distance. For both the cases at X=5h and X=10h downstream distances the peak Nu/Nu_0 values have been noticed in between two adjacent cylinders at Y= ±0.5h. Areas which are

blocked by the cylinders indicating lower Nu/Nu_0 corresponding to the area in between cylinders. As fresh air has been blocked by the cylinders approaching towards the hot surface, areas over the plate behind the cylinders has lower Nu/Nu_0 values compared to the area in between cylinders [3]. This hints that there is a lack of fresh cold air approaching the hot surface of the plate behind the cylinders and a less interaction of flow field on those areas compared to the area in between cylinders results in diminishing the local heat transfer rate.
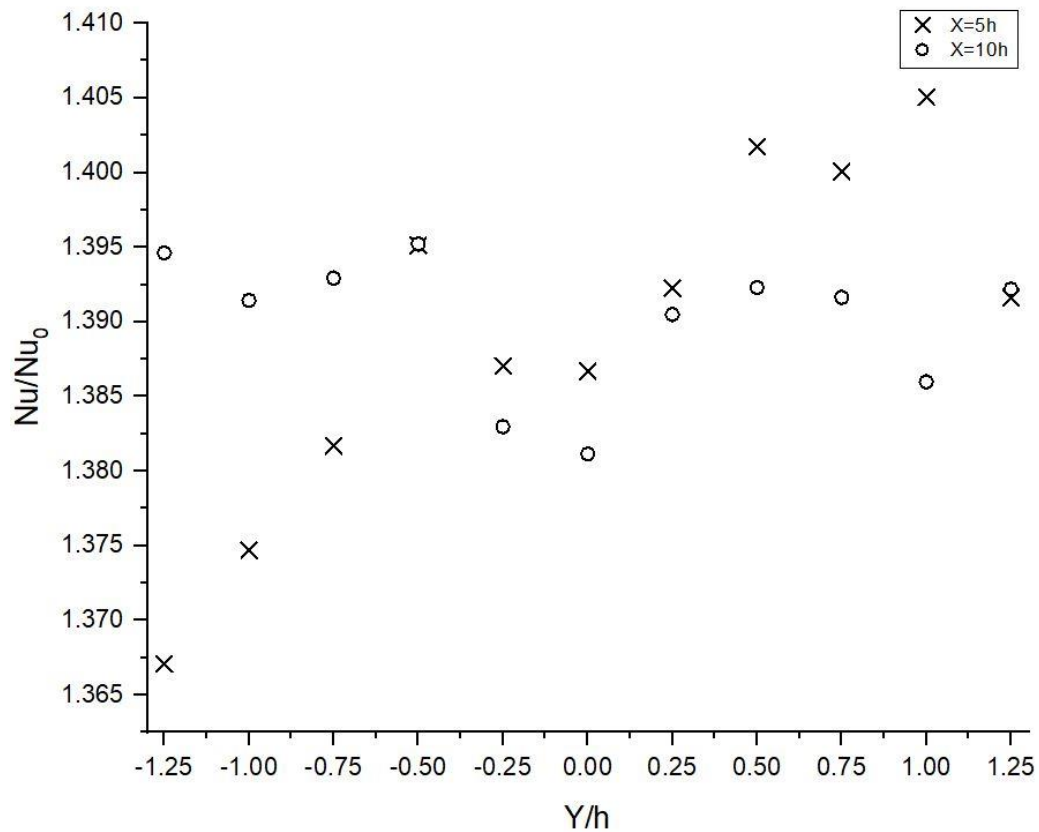

Figure 3.2: The cross-sectional Nu/Nu_0 profile at (a) $X=5h$, (b) $X=10h$ downstream.

In case of practical appliance, such as solar panel cooling, the entire panel needs to be considered. Therefore, the average *Nu/Nu₀* has importance over localized *Nu/Nu₀*. To see the variation of average *Nu/Nu₀* over the flat plate on various downstream distances averaged normalized Nusselt number is plotted in figure 3.3. The largest average Nu/Nu_0 value is observed right behind the array of cylinder until X=2h where the intense velocity fluctuation and higher turbulence intensity zone appears. Farther downstream, X=10, the heat transfer enhancement starts to decrease. This is likely to occur as turbulent flow behind the cylinder array starts to decay. To understand the heat transfer behavior from an array of cylinder over flat plate we need to look at the flow characteristics in the next section.
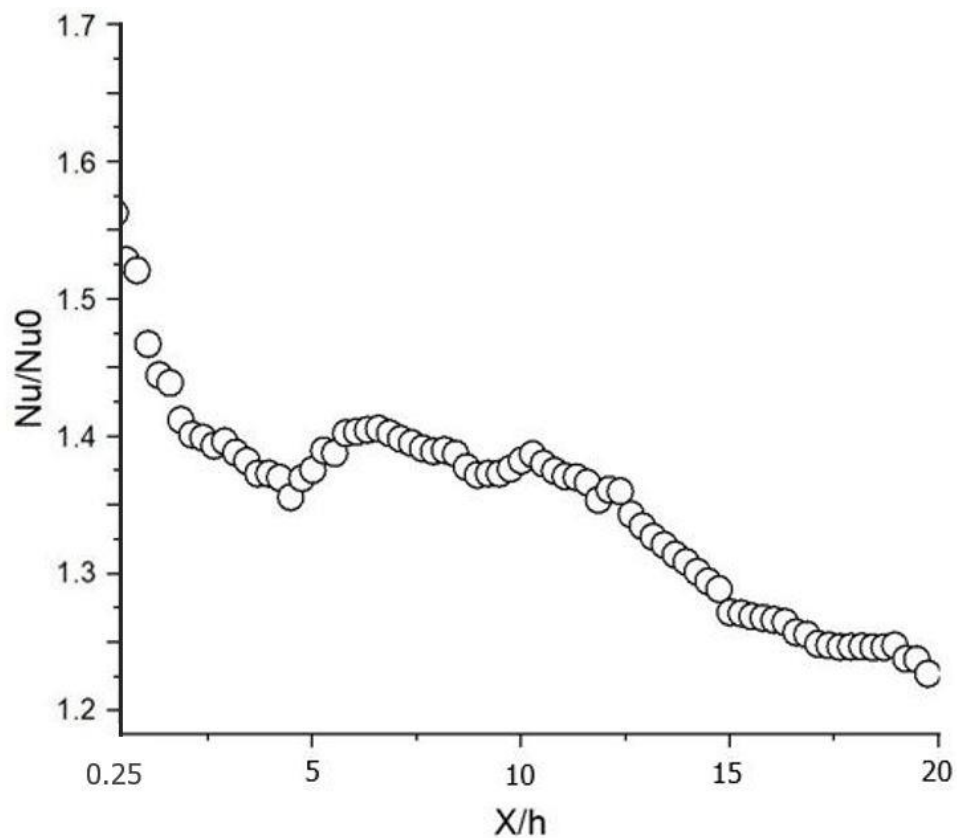

Figure 3.3: Normalized average (over Y= ±1.25h) Nusselt number, *Nu/Nu₀,* distribution downstream of the array of cylinders.

3.2 Flow Characteristics

3.2.1 Velocity Profile

Heat transfer enhancement is affected by stream-wise velocity downstream the flow. Figure 3.4 represents the velocity profile at YZ plane where time-averaged stream -wise velocity is normalized by free stream velocity U_∞. The uncertainty of stream-wise velocity was around 0.31 m/s and the uncertainty of mean $\bar{U}/U_\infty$ was approximately 0.044. The dotted cylinders denote the center three cylinders of the cylinder array. Intense velocity fluctuation is being observed in between cylinders at X=5h downstream distance Figure 3.4 (a). Here fresh air approaches faster towards the hot surface resulting the interaction of flow field in between cylinders. As flow interference between successive cylinders is quite strong at small separation ratio [4].

(a)
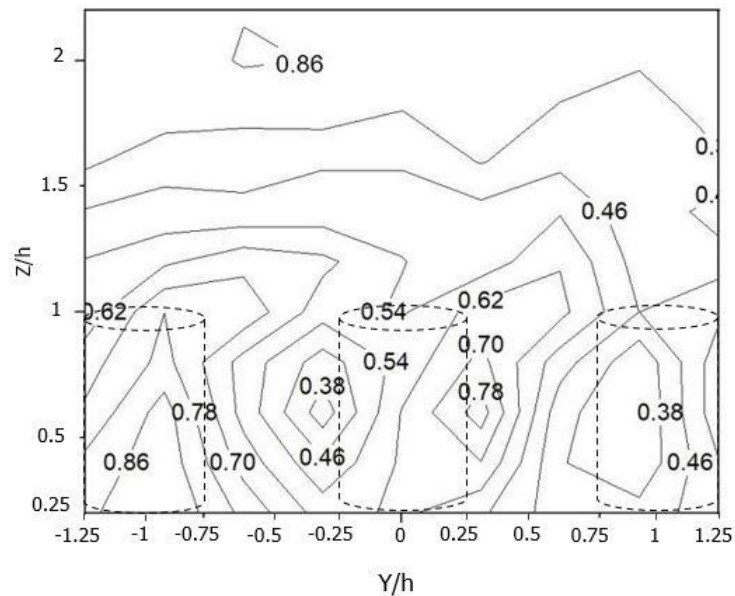
(b)
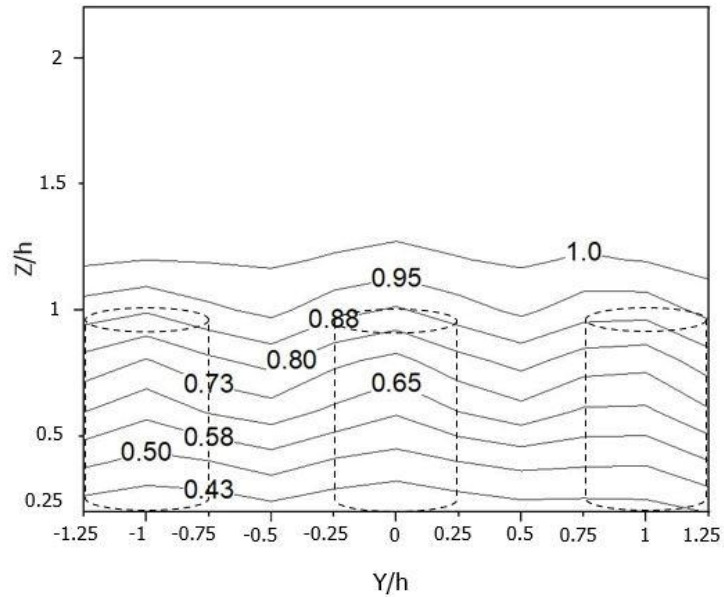
Figure 3.4: Normalized stream-wise time-averaged velocity ($\bar{U}/U_\infty$) at YZ plane at (a)

X=5h and b) X=10h downstream

At X=10h downstream distance as we are moving away from the array of cylinders

boundary layer thickness increases gradually resulting the less interaction of flow field

hence decrease in Nu/Nu_0.

3.2.2 Turbulent Intensity

The turbulent intensity is another important parameter that plays a significant role dictating

the convicting heat transfer [5]. Figure 3.5 depicts the normalized turbulence intensity

where local turbulence fluctuation has been normalized by free stream time-averaged

velocity. Figure 3.5 (a) represents the normalized turbulent intensity profile at X=5h

downstream distances whereas figure 3.5 (b) represents the normalized turbulent intensity

profile at X=10h downstream of the cylinder array. The dotted cylinders denote the center

three cylinders of the cylinder array located at X=0h on the flat plate. The uncertainty estimated for Turbulent intensity is approximately 0.0043. Tu value more than 3% is considered to have good effect on flow over a flat plate [6].As can be seen, the turbulent intensity near the plate (0.25h) is 0.039 which roughly coincide with the higher Nu/Nu_0 zone in Figure 3.3 just after crossing the cylinder row and also with near surface fluctuating stream-wise velocity Figure 3.5. There is a declination of the turbulent intensity as we are moving away from the cylinder. This declination of turbulence intensity occurs due to the gradual increase in boundary layer thickness away from cylinder row [7]. Figure 3.5.(b) follows the decreasing pattern in Nu/Nu_0 over the flat plate away from the cylinder array in Figure 3.3. It can be drawn from this part of the discussion is that the large area of the Tu over the flat plate could significantly contribute to the local heat transfer rate.

(a)
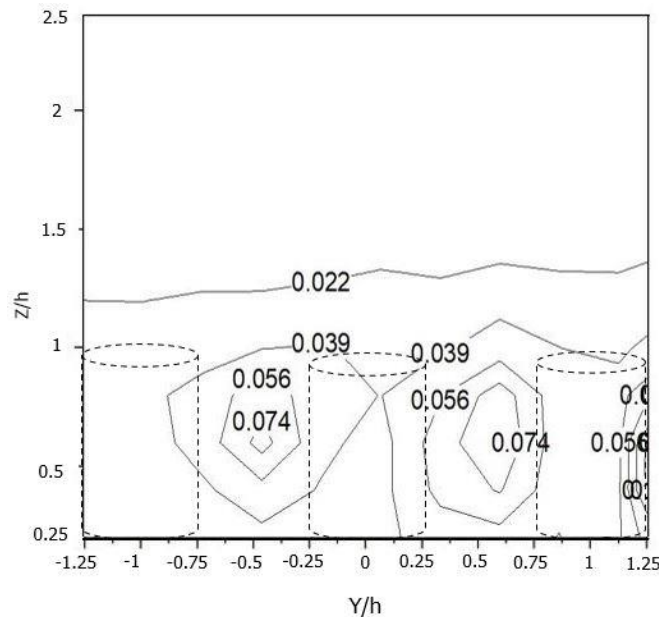
(b)
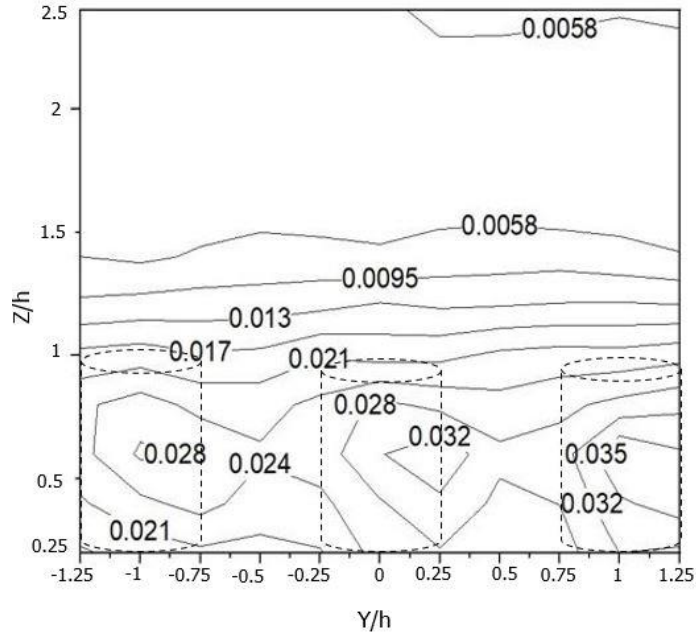
Figure 3.5: Normalized stream-wise turbulent intensity (U_{rms}/U_∞) at YZ plane at (a)

X=5h and b) X=10h downstream

3.2.3 Taylor Microscale

Dissipative end of the turbulence energy cascade is represented by the Taylor microscale

[8]. Taylor microscale can describe the small eddies in the turbulent hence is also of interest

in heat convection. Figure 3.6 represents the stream-wise Taylor microscale normalized by

the cylinder height (20mm) at (a) X=5h and (b) x=10h downstream distance of the cylinder

array. The dotted cylinders denote the center three cylinders of the cylinder array located

at X=0h on the flat plate. The uncertainty estimated for the Taylor microscale is around

0.045. In Figure 3.6 Taylor microscale has its smaller value adjacent to the plate and

increases quickly with increasing z (height) around the top end of the cylinder array away

from the flat plate which follows the same patters as turbulent intensity. In Figure 3.6.

higher Tu value has been observed in between cylinders and near the surface of the heated plate. A stronger turbulence level can sustain a higher dissipation rate and thus a smaller Taylor microscale has been noticed into those area[5]. A decrease in Taylor microscale has been noticed as we move more towards top of the cylinder array more toward the free stream. The effect of Taylor microscale on Nu/Nu_0 based on the contour plots is difficult to define. Thus, in next section we focused on multiple linear regression analysis.

(a)
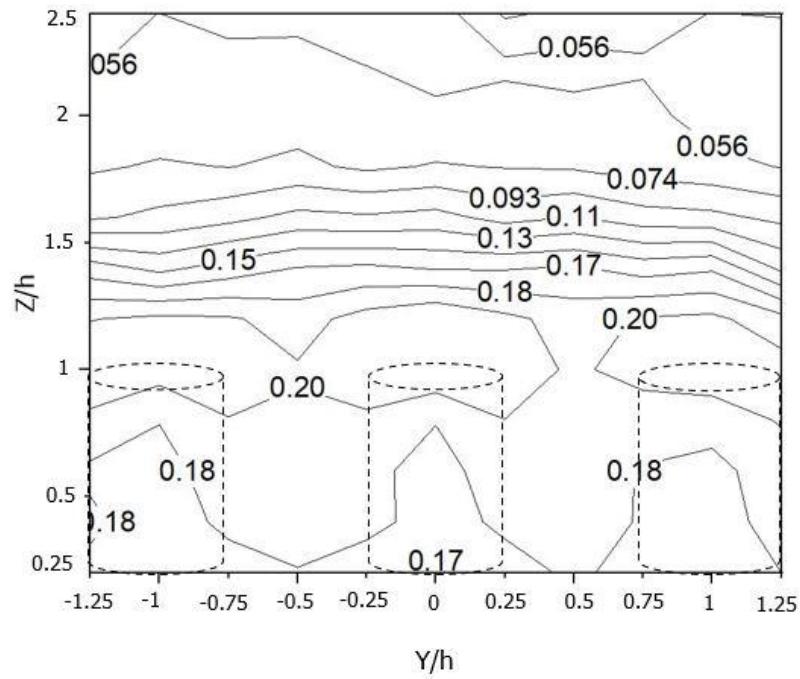
(b)
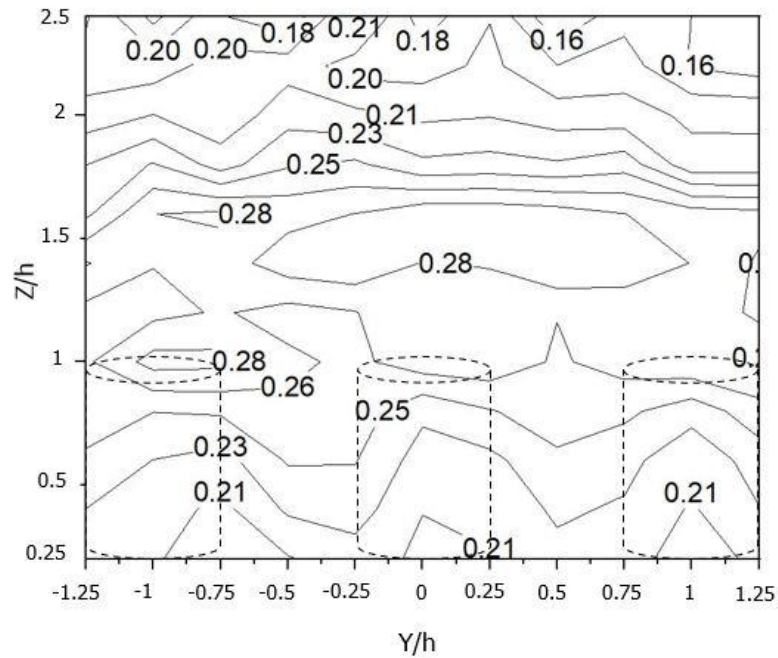
Figure 3.6: Normalized stream-wise Taylor microscale λ/h at YZ plane at (a) X=5h and

b) X=10h downstream

3.3. Regression Analysis

From the heat transfer enhancement results and the flow characteristics described in

aforementioned sections it can be said that the heat transfer augmentation is induced by

multiple flow mechanism. Hao et al [5] investigated the effect of delta winglet on flat plate

and according to their study the total turbulence fluctuation has the largest effect on heat

transfer followed by the velocity towards the flat plate. Thus, the individual effect of the

flow properties on the heat transfer enhancement are of interest in the current study. To

find out the weight of stream-wise velocity by the time-averaged free-stream velocity by

the time-averaged free-stream velocity and local stream-wise turbulent intensity

normalized by time-averaged free-stream velocity on heat transfer augmentation multiple

linear regression analysis has been performed. To understand the overall impact of this parameters on heat transfer over a flat plate irrespective of their downstream distances, a regression analysis has been performed including both sets of data taken at X=5h and x=10h downstream distance, spanning the cross-section defined by $Y=\pm1.25h$, and at $Z=0.25h$ (closest to the surface point). The raw data of the regression analysis are plotted in the Figure 3.7.

The result of the regression analysis is summarized in the table 3.1. Only values closest to the plate at Z=0.25h were employed in the analysis. The reason behind this is to study the effect of the local flow properties impact on heat convection from the heated flat plate which we considered of having the largest impact on Nu/Nu_0.

(a)

$$\overline{U}/U_\infty$$

(b)
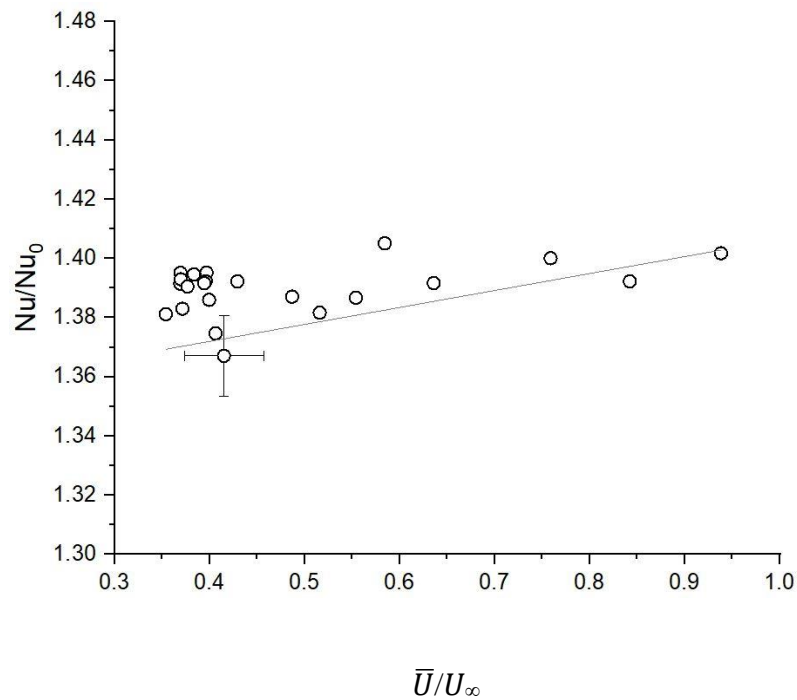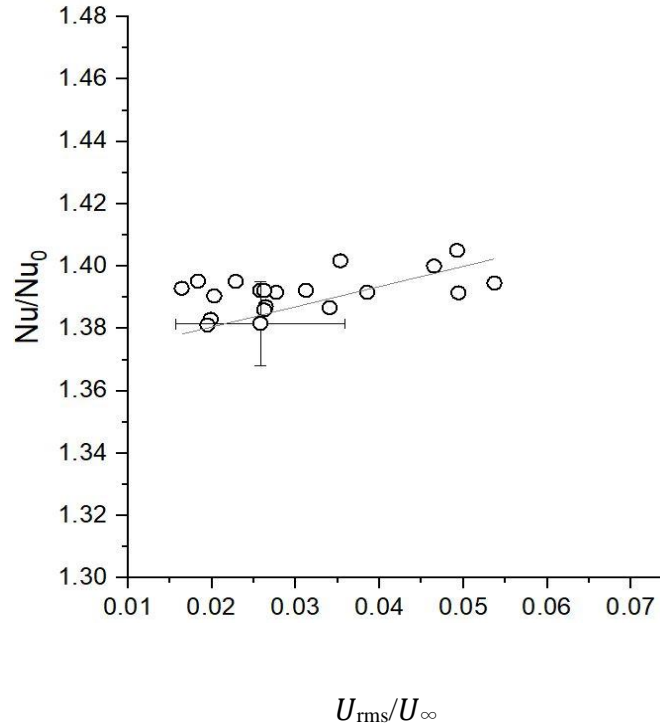
U_{rms}/U_∞

Figure 3.7: *Correlating* normalized (a) stream-wise velocity, $\overline{U}/U_\infty$ and local stream-wise turbulent intensity, U_{rms}/U_∞, with *Nu/Nu₀* irrespective of downstream distances (X=5h and X=10h) Y=±1.25h, and Z=0.25h. respectively. R-square value *of* $\overline{U}/U_\infty$ is 0.439, *R*-square values of U_{rms}/U_∞, is 0.652.

Table 3.1. Multiple linear regression results

Parameter	$\overline{U}/U_\infty$	U_{rms}/U_∞	λ/h
Standardized regression coefficient ($\beta_j{}^{std}$)	0.439	0.652	0.036

The absolute value of the standardized regression coefficient ($\beta_j{}^{std}$) has been used in the Table 3.1 to determine the weight of each parameter on heat transfer augmentation. It is noticeable from Figure 3.7 that, among the studied parameters streamwise velocity $\bar{U}/U_\infty$ has the largest influence on heat transfer enhancement as there is a higher slop between $\bar{U}/U_\infty$ and Nu/Nu$_0$. The R square value for streamwise velocity $\bar{U}/U_\infty$ is 0.439 which denotes that it has a moderate co-relation with the independent variable Nu/Nu$_0$. In this case, R square value is around 0.45 which indicates moderate co-relation between independent and dependent variable [9]. It concludes from Figure 3.7 that as the slop between Nu/Nu$_0$ and $\bar{U}/U_\infty$ is higher if streamwise velocity increases Nusselt number will also increase. This indicates the continuous flow of air over flat plate which helps faster and effective cooling of the heated plate. From Figure 3.7 is noted that, the next effective parameter is turbulent intensity U_{rms}/U_∞which ensures the bringing of cool air to the plate and carry away hot air from the heated plate thus resulting in significant cooling of the heated surface. The R square value from Table 3.1 for Turbulent intensity U_{rms}/U_∞ is 0.652 which denotes that it has a strong co-relation with the independent variable Nu/Nu$_0$ as R square value is more than 0.50 indicating stronger co-relation. It concludes from Figure 3.7 that if turbulent intensity increases Nusselt number will also increase. The last ranked parameter is Taylor microscale λ/h which has not so obvious effect on heat transfer augmentation. Only possible conclusion can be losses of influence on heat transfer if the eddy is too small. Moreover, the overall R-square value (irrespective of individual parameters) is 0.695 which ensures that an array of cylinder over a flat plate can be beneficial in heat transfer augmentation.

3.4 Conclusion

This study experimentally investigated flow downstream of an array of finite height cylinders and the effect on forced convection from a flat surface at Re 4700, gap between cylinders, g=2d and aspect ratio of h/d=2 (height of each cylinder 20mm and diameter 10mm). The heat transfer rate in terms of the normalized Nusselt number, Nu/Nu_0, was experimentally studied with the help of various flow properties like stream-wise time-averaged velocity, stream-wise turbulence intensity and Taylor microscale. Maximum peak Nu/Nu_0 has been observed in between cylinders just after crossing the cylinder array which coincides with the location of maximum turbulent intensity and intense velocity fluctuation zone. Also, average Nusselt number over the entire plate shows promising heat transfer enhancement. An overall multiple linear regression has also been performed to find out the most effective flow properties behind heat transfer augmentation. According to the regression analysis, the largest influential parameter is stream wise velocity followed by streamwise turbulent intensity. This indicates that a larger local wind velocity and higher turbulent intensity induced by an array of finite height cylinders over a flat plate can results in promising heat transfer augmentation.

Reference

[1] García-Villalba, M., Palau-Salvador, G., & Rodi, W. (2014). Forced convection heat transfer from a finite-height cylinder. Flow, turbulence and combustion, 93(1), 171-187.

[2] Silva, A. L. E. (2014). Convection heat transfer around a single row of cylinders. Computational Thermal Sciences, 6 (6): 477–492.

[3] Yang, Y., Ting, D. S. K., & Ray, S. (2020). Heat transfer enhancement of a heated flat surface via a flexible strip pair. International Journal of Heat and Mass Transfer, 159. 120-139.

[4] Wei, Y. K., & Hu, X. Q. (2017). Two-dimensional simulations of turbulent flow past a row of cylinders using lattice Boltzmann method. International Journal of Computational Methods, 14(01), 1750002.

[5] Wu, H., Ting, D. S. K., Ray, S. (2018). The effect of delta winglet attack angle on the heat transfer performance of a flat surface. International Journal of Heat and Mass Transfer, 120, 117–126.

[6] Iakovidis, F., Fartaz, A., David S-K, T., Ray,S.,(2013). Air Cooling of PV Panels. University of Windsor.

[7] Cheng, M., & Moretti, P. M. (1988). Experimental study of the flow field downstream of a single tube row. Experimental Thermal and Fluid Science, 1(1), 69-74.

[8] Taylor, G. I (1938). The spectrum of turbulence, Proc. R. Soc. London. Ser. Math. Phys. Sci., pp. 476–490.

[9] Moore, D. S., Notz, W. I, & Flinger, M. A. (2013). The basic practice of statistics (6th ed.). New York, NY: W. H. Freeman and Company. Page (138).

CHAPTER 4

Conclusion and Recommendation

4.1 Conclusion

This study experimentally investigates the effect of a row of finite-height cylinders placed over a flat plate on heat transfer augmentation. 13 number of cylinders had been used at Re=4700 in a row maintaining gap spacing between each cylinder as 2d where each cylinder had a height of 20 mm and a diameter of 10mm resulting aspect ratio (h/d) of 2.

In case of heat transfer augmentation, the maximum peak *Nu/Nu0* was being observed just after crossing the cylinder and gradually decreases by moving towards downstream distances. The highest average Nusselt number was noticed over the entire plate indicating significant heat transfer enhancement.

 The flow properties revealed that:

- At x=5h downstream distances as faster moving fluid approaches the heated plate, the near surface higher turbulent intensity and interaction of flow field has been observed causing the thinning of boundary layer thickness. Near the plate, Tu value adjacent to the plate was 0.039 and average streamwise velocity near the plate(0.25h) is around 0.6.
- At X=10h downstream distance as we are moving away from the array of cylinders boundary layer thickness increases gradually resulting the less interaction of flow field hence decrease in Tu value has been observed. The average near surface Tu value at x=10h is around 0.025. and the near plate streamwise velocity is 0.43.

- By moving further away from the cylinder row, Turbulent intensity decreases with less interaction of flow field which coincides with the decreasing pattern of normalized Nusselt number *Nu/Nu₀* away from the cylinders.

A multiple linear regression analysis was performed with respect to normalized Nusselt number, Nu/Nu_0 by considering stream-wise-velocity $\overline{U}/U_\infty$, Turbulent intensity $Urms/U\infty$ and Taylor microscale λ/h. The analysis supports that stream-wise velocity is the most effective parameter followed by turbulent intensity in case of heat transfer augmentation. The analysis also has an overall R-square value of 0.695 indicating promising heat transfer augmentation from a row of cylinders over a flat plate. Finally, it can be concluded that, an overall effective heat transfer can be achieved from a row of cylinder over a flat plate.

4.2 Recommendation

Array of cylinders over a flat plate are very promising in convective heat transfer enhancement. This study examined the effect of a single row of cylinder over a flat plate at only two downstream distances (X=5h and X=10h). The flow characteristics at different downstream distances can be studied to support the existing heat transfer data. Also, by changing other parameters like cylinder aspect ratio further experimentation can be conducted. Finite height cylinders with multiple arrays over a flat plate can also be practically examined.

APPENDICES

Appendix A. Uncertainty Analysis

For obtaining the instantaneous velocity data we consider two parameters like the uncertainty of bias (B) and precision (P).The total uncertainty can be obtained as follows:

$$E = \sqrt{B^2 + P^2} \qquad\qquad\qquad (A\text{-}1)$$

Uncertainty of U_i

At characteristic point of Y/h=0 & Z/h=1.5, the bias uncertainty of instantaneous velocity is influenced by the process of calibration (0.194 m/s), linearization (0.097 m/s), A/D resolution (0.078 m/s), and probe positioning (0.015 m/s). The bias uncertainty of the instantaneous velocities is as follows:

$$B(U_i) = \sqrt{0.194^2 + 0.097^2 + 0.078^2 + 0.015^2} = 0.231 \text{ m/s} \qquad (A\text{-}2)$$

The hotwire is rested to freestream and velocity is measured 20 times, by doing this process the precision of uncertainty velocity is obtained. For every measurement, $N = 10^6$ points were recorded, and P follows the Student's distribution method with a confidence interval of 95% (by choosing M as 2×10^7, the t value is 1.960).

$$P(U_i) = 0.11 \text{ m/s} \qquad\qquad\qquad (A\text{-}3)$$

Then the total uncertainty of U_i becomes:

$$E(U_i) = \sqrt{B(U_i)^2 + P(U_i)^2} = \sqrt{0.20^2 + 0.11^2} = 0.228 \text{ m} \qquad (A\text{-}4)$$

Uncertainty of $\bar{U}$

The mean velocity (7 m/s) bias uncertainty takes the same value as the bias uncertainty of the instantaneous velocity.

$$B(\bar{U}) = B(U_i) = 0.231 \ m/s \tag{A-5}$$

The precision uncertainty of the mean velocity is obtained by resetting the hotwire to the typical position and measuring the velocity for 20 times (t is 2.08). The precision of $\bar{U}$ can be expressed as:

$$P(\bar{U}) = 0.2 \ m \tag{A-6}$$

From the above equations, the uncertainty of $\bar{U}$ can be obtained as:

$$E(\bar{U}) = \sqrt{B(\bar{U})^2 + P(\bar{U})^2} = \sqrt{0.231^2 + 0.20^2} = 0.31 \ m/s \tag{A-7}$$

Uncertainty of u_{rms}

The bias uncertainty in u_{rms} can be estimated:

$$B(u_{rms}) = 0.0112 \ m/s \tag{A-8}$$

By measuring the characteristic points for 20 times, the precision of u_{rms} is obtained to be:

$$P(u_{rms}) = 0.0283 \ m/s \tag{A-9}$$

Then the uncertainty of u$_{rms}$ is:

$$E(u_{rms}) = \sqrt{B(u_{rms})^2 + P(u_{rms})^2}$$

$$= \sqrt{0.01125^2 + 0.0283^2} = 0.0304 \, m/s \qquad \text{(A-10)}$$

Heat Transfer

The temperature distribution is captured by the thermal camera which is calibrated by a thermocouple which has a bias uncertainty of 0.5°C. The top surface temperature is captured by the thermal camera 10 times giving raise to the precision uncertainty of 0.37°C. Using the propagation of the uncertainty, each parameter's uncertainty involved in the heat transfer can be estimated.

$$E(\dot{Q}_{Total}) = \sqrt{[\frac{\partial \dot{Q}_{Total} E(T_{Top})}{\partial T_{Top}}]^2} = \frac{K_{PTFE} A}{t_{PTFE}} E(T_{Top}) \qquad \text{(A-11)}$$

$$E(\dot{Q}_{radiation}) = \sqrt{[\frac{\partial \dot{Q}_{radiation} E(T_{Top})}{\partial T_{Top}}]^2} = 4\varepsilon\sigma A T_{Top}^3 E(T_{Top}) \qquad \text{(A-12)}$$

$$E(\dot{Q}_{convection}) = \sqrt{\left[\frac{\partial \dot{Q}_{convection} E(\dot{Q}_{Total})}{\partial \dot{Q}_{Total}}\right]^2 + \left[\frac{\partial \dot{Q}_{radiation} E(\dot{Q}_{radiation})}{\partial \dot{Q}_{radiation}}\right]^2}$$

$$E(\dot{Q}_{convection}) = \sqrt{[E(\dot{Q}_{Total})]^2 + [E(\dot{Q}_{radiation})]^2} \qquad \text{(A-13)}$$

Uncertainty of each parameter was calculated as per equation A-11 and A-15 and calibration error of the probe. The uncertainty of Nu/Nu0 is 0.622. Two tables separate tables below contain the uncertainties of studied parameters.

Table A.1. Typical uncertainties of mean velocities and their respective root-mean squares uncertainties.

Parameter	$\bar{U}$	$\bar{V}$	U_{rms}
Uncertainty	0.31	0.035	0.0304

Table A.2.Representative uncertainties of studied parameters

Parameter	Nu/Nu_0	$\bar{U}/U_\infty$	U_{rms}/U_∞	λ/h
Uncertainty	0.0622	0.0443	0.0043	0.045

VITA AUCTORIS

NAME: Saarah Akhand

PLACE OF BIRTH: Rangpur, Bangladesh.

YEAR OF BIRTH: 1994

EDUCATION: Military Institute of Science and Technology
                  (MIST), B.Sc., Dhaka, Bangladesh, 2017

                  University of Windsor, M.Sc., Windsor, ON,
                  2021